Catalysis Today 441 (2024) 114879

Contents lists available at ScienceDirect

Catalysis Today

journal homepage: www.elsevier.com/locate/cattod

Tailoring selective de-hydroxylation/hydrogenation reactions of bio-based aldaric acids towards adipic acid derivatives by Re catalyst metal–support interactions

Florian M. Harth [a,1], Maja Gabrič [a,b,1], Janvit Teržan [a], Brigita Hočevar [a], Sašo Gyergyek [c], Blaž Likozar [a,d,e], Miha Grilc [a,b,*]

[a] Department of Catalysis and Chemical Reaction Engineering, National Institute of Chemistry, Hajdrihova 19, Ljubljana 1000, Slovenia
[b] University of Nova Gorica, Vipavska Cesta 13, Nova Gorica 5000, Slovenia
[c] Department for Materials Synthesis, Jožef Stefan Institute, Jamova 39, Ljubljana 1000, Slovenia
[d] Faculty of Polymer Technology, Ozare 19, Slovenj Gradec 2380, Slovenia
[e] Pulp and Paper Institute, Bogišićeva 8, Ljubljana 1000, Slovenia

ARTICLE INFO

Keywords:
Heterogeneous catalysis
Rhenium
Deoxydehydration
Oxidation state
Renewable Resources
Bifunctional catalyst

ABSTRACT

Rhenium-based catalysts are highly active in the catalytic deoxydehydration (DODH) reaction, which results in selective dehydroxylation of vicinal diols to unsaturated products. Hereby, DODH combined with subsequent hydrogenation, is applied to upgrade biomass-derived mucic acid towards renewable adipates using supported Re catalysts. The influence of different support materials, as well as the effect of catalyst pretreatment conditions, were examined in our study. The results strongly suggest that only C and TiO_2 serve as suitable supports for Re to achieve noticeable DODH activity. Furthermore, reductive pre-treatment protocol crucially affects DODH activity. This pre-treatment is essential for achieving yields of up to 88 % for fully dehydroxylated products at low reaction temperature of 120 °C with methanol as reducing agent. Most notably, DODH activity depends on the co-existence of metallic and high-valent Re sites, as catalyst characterization indicates. Particle growth during (reductive) thermal treatment probably increases the formation of bifunctional sites. A corresponding bifunctional reaction mechanism of the DODH on monometallic Re catalysts is proposed, which can explain the experimental results.

1. Introduction

A crucial aspect for the transition towards a more sustainable chemical industry in the replacement of fossil resources by renewable resources such as lignocellulosic biomass [1,2]. The conversion of lignocellulose to industrially demanded chemicals has been the focus of countless studies exploring biotechnological, thermal, and chemo-catalytic pathways [3–7]. An important and attractive group of molecules to target are monomers for the polymer industry [8,9]. A highly sought-after molecule is adipic acid (AA), one of the monomers for the production of polyamides and polyesters. In recent literature, different routes towards AA have been reported [10–13], among them a pathway making use of the Re-catalyzed deoxydehydration (DODH) reaction [14,15].

The DODH in this case is applied to selectively dehydroxylate hexose-derived aldaric acids to yield AA (or its esters). This process was first developed with homogeneous catalysts [16,17], however, recently, the successful application of solid catalysts has also been observed for the production of AA and its derivatives [18–22]. In Fig. 1 the typical reaction pathway and (intermediate) products are shown, as observed in our previous study [19]. Only esterified products are obtained due to rapid esterification of the reactant with the solvent and reducing agent methanol.

Rhenium plays a crucial role in catalyzing the DODH reaction of aldaric acids and both monometallic and bimetallic solid catalysts relying on Re as the primarily active DODH site have been used. In particular, in recent studies by Deng *et al.* [21] and Jang *et al.* [22,23] Re was combined with either Pt, Pd or Ir and both research teams concluded

* Corresponding author at: Department of Catalysis and Chemical Reaction Engineering, National Institute of Chemistry, Hajdrihova 19, Ljubljana 1000, Slovenia.
E-mail address: miha.grilc@ki.si (M. Grilc).
[1] Both authors contributed equally

https://doi.org/10.1016/j.cattod.2024.114879
Received 31 January 2024; Received in revised form 24 May 2024; Accepted 5 June 2024
Available online 7 June 2024

that oxidic Re species are the main active DODH sites in the DODH of aldaric acids while the additional noble metal, present in metallic state, further promotes the DODH reaction and primarily catalyzes the subsequent hydrogenation of initially formed unsaturated compounds into saturated AA. This is also in agreement with the concept proposed by Tomishige *et al.* [24] regarding the general role of the Re oxidation state in DODH reactions. However, our own research on the DODH of mucic acid to adipates [19] showed that a beneficial effect of reductive catalyst pretreatment can be observed when using monometallic Re catalysts under similar reaction conditions. DODH product yield in this case nearly doubled when reducing the commercially available Re/C catalyst under H_2 for 3 h at 400 °C prior to the catalytic experiment, indicating that also metallic or low-valent Re species must play an important role. A similar effect was also reported by Sandbrink *et al.* [25]. However, also the possible agglomeration of Re under thermal treatment must be considered and it is conceivable that Re particle size may also influence catalytic activity. Thus, the investigation of the effect of catalyst pretreatment is one of the objectives of this study, targeted at understanding how Re oxidation state as well as dispersion can be tuned to optimize DODH activity.

Moreover, the influence of the support material on the reaction is investigated. Based on the available literature, different materials such as TiO_2 [25], ZrO_2 [26], CeO_2 [27], zeolites [28] or carbon [19] have been presented as well-suited supports for monometallic Re [29,30]. While a general influence of the support material is evident from all of the aforementioned studies, the trends and the reasons for the differences in DODH activity are not always clear. It has been speculated that also in this case the Re oxidation state is highly relevant and that Re reducibility may be a critical influencing factor [20]. Thus, the focus of this study is to gain a deeper understanding into how the Re sites are influenced by different support materials and how this, in turn, governs catalytic activity, contributing to the field's understanding of biomass conversion processes and catalytic optimization.

2. Materials and methods

2.1. Catalysts and pre-treatment

All catalysts used in this study are commercially available and were purchased from Riogen, USA. The following materials were tested: Re/C, Re/TiO_2, Re/ZrO_2, Re/SiO_2, Re/Al_2O_3, Re/H-Y zeolite and Re/H-ZSM-5 zeolite. They are all in power form and each has a loading of 5.0 wt% Re. Directly prior to each catalytic experiment as well as characterization procedure (unless stated otherwise), the respective catalyst was subjected to a reductive pre-treatment procedure carried out ex-situ in a tubular furnace. In the standard procedure, the catalyst was heated to the temperature of 400 °C (ramp of 5 K min^{-1}), at which it was kept for 3 h under a flow of H_2 (0.2 L min^{-1}). During the transfer of the reduced catalysts to the characterization or experimental apparatus the materials were stored in inert atmosphere, however during the actual manipulation the exposure to air could not be omitted which could cause partial reoxidation of Re.

For the Re/C catalyst the influence of the reductive pre-treatment was investigated, for which the standard procedure was adjusted in several ways. On the one hand, reduction time at 400 °C was increased to 20 h under H_2 purge, with an additional experiment during which after 3 h the gas was switched from H_2 to N_2 for the remaining 17 h. On the other hand, an experiment with reduction at 250 °C under H_2 for 20 h was conducted.

2.2. Catalytic experiments and product analysis

All catalytic experiments were conducted in a Parr Series 5000 parallel system consisting of six stainless steel batch reactors with a volume of 75 mL. Each reactor was equipped with stirrer, heater, gas inlet, dip tube, pressure gauge and thermocouple for independent control of each vessel. In a typical experiment, 0.33 mmol of the reactant mucic acid (Sigma Aldrich, 97 %) and 45.0 mL methanol (J.T. Baker, 99.8 %) were used as reactant mixture to which 140 mg of the pre-reduced, supported Re catalyst were added. The reactor vessel was loaded, purged and pressurized with N_2 (Messer, 5.0) to 0.5 MPa and heated to the desired reaction temperature of 120 °C. The reactor was continuously stirred at 700 rpm and the reaction allowed to proceeded for 72 h, during which liquid-phase samples were taken repeatedly. Product analysis and quantification was conducted by GC-MS as described in detail in our previous article [19], however the different hexenedioate isomers are summarized as one product category here.

2.3. Catalyst characterization

N_2 physisorption experiments at 77 K were performed for all fresh catalyst to obtain adsorption and desorption isotherms. From those, the respective specific surface area (using the BET model) and specific pore volume was determined. The measurements were performed on a Micromeritics ASAP 2020 analyzer, degassing at 200 °C to 3 μm Hg for 17 h with 70 mg of the sample.

For temperature-programmed reduction with H_2 (H_2-TPR) was performed with the Micromeritics Autochem II 2920 (Micrometrics, Norcross, GA, USA). The sample, used as supplied, was first pretreated to 200 °C in Ar with 10 °C min^{-1} and then exposed to a 5 % H_2/Ar at a flow rate of 20 mL min^{-1}. The sample was then heated at a rate of 5 °C min^{-1} to 500 °C and maintained at this temperature for 30 min. During the reduction process, a mass spectrometer was used to monitor and quantify H_2 consumption and desorbed gasses. After the reduction, the

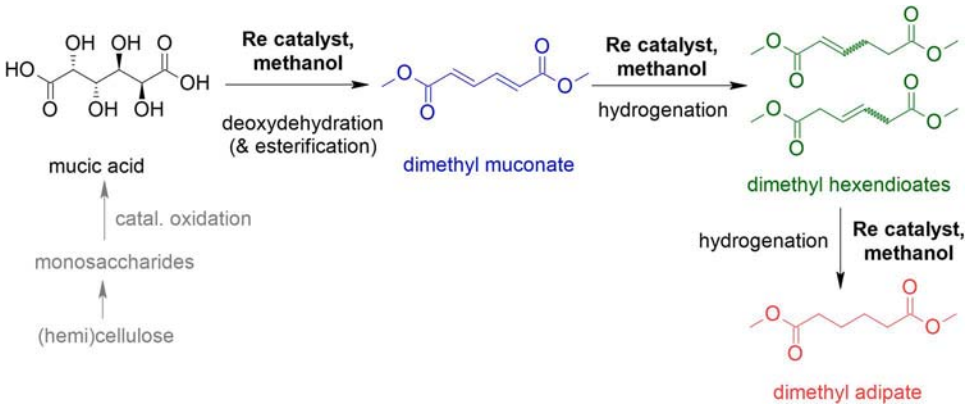

Fig. 1. Scheme of the catalytic conversion of the biomass-derived aldaric acid mucic acid over Re-containing catalysts in methanol. The unsaturated product dimethyl muconate is formed via catalytic deoxydehydration and can be subsequently hydrogenated into dimethyl hexendioates and further into dimethyl adipate.

sample was cooled to 40 °C and purged with Ar gas at a flow rate of 20 mL min^{-1}.

X-ray photoelectron spectroscopy (XPS) was applied to observe the oxidation state of Re on different supports after reduction. The analysis was performed with the PHI VersaProbe 3 AD (Phi, Chanhassen, US), which uses a monochromatic Al Kα X-ray source. For charge neutralisation, the charge of the sample was attenuated with two beams (electrons and ions). The peak shift caused by the neutralisation was corrected by shifting the peaks of the random carbon species to 284.8 eV. The survey spectra were measured at a transit energy of 224 eV with a step of 0.8 eV. The high-resolution spectra were measured with a transit energy of 50 eV and a step of 0.05 eV. Two sweeps were performed for the survey spectra, while 25 sweeps were performed for the high-resolution spectra. Spectral deconvolution was performed using Multipak software.

For transmission electron microscopy (TEM), dry samples were dispersed in isopropanol and deposited on a carbon-coated Cu specimen grid. Jeol JEM2100 transmission electron microscopes (TEM) operated at 200 kV and a Cs-corrected Jeol ARM 200CF STEM scanning transmission electron microscope (STEM) operated at 80 kV were used to observe the samples deposited on a copper-grid-supported lacy carbon foil. During the analysis High-angle annular dark-field (HAADF) and brigh-field (BF) detectors were used simultaneously at 68–180 and 10–16 mrad collection semi-angles, respectively. To determine the empirical size distribution of the Re particles, the area of the particles on the TEM image was measured. The particle size dTEM is given as an equivalent diameter, i.e., the diameter of a circle having the same surface area as the imaged particle. Only clearly visible Re nanoparticles were takin into account for size distribution, agglomerates and atoms/clusters were not taken into account.

3. Results and discussion

3.1. Influence of the support material

A series of catalysts containing 5 wt% Re on different support materials was tested in the catalytic DODH of mucic acid in methanol at 120 °C. The results presented in Fig. 2 show considerable differences regarding their catalytic behavior.

By far the highest DODH activity was observed over Re/C, the catalyst reported as a well-suited catalyst for this reaction system in our previous study [19]. In total more than 65 % of DODH products were obtained after 72 h, of which about half was the initially formed, twice unsaturated product dimethyl muconate. A similar amount was already further hydrogenated to dimethyl hexenedioates, which contain one fewer double bond. This shows that the Re/C catalyst is able to catalyze both the DODH reaction as well as the first hydrogenation step (see also Fig. 1). However, the further hydrogenation to fully saturated dimethyl adipate could only be observed in negligible amounts, which requires harsher reaction conditions, especially higher reaction temperature or the presence of a stronger reducing agent (gaseous H_2) at 120 °C.

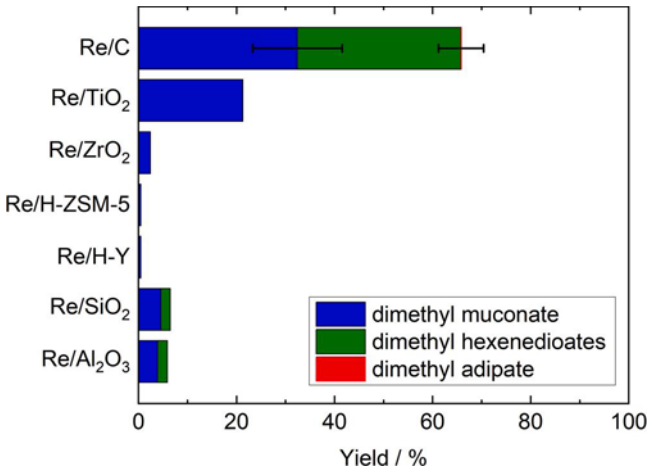

Fig. 2. Yield of dehydroxylation products obtained over different supported Re catalysts. Reaction conditions: 140 mg mucic acid, 45.0 mL methanol, 140 mg catalyst, 120 °C, 5 bar N_2, 72 h. Each catalyst underwent a pre-reduction process for 3 hours at 400 °C in the presence of a hydrogen flow. Note that for Re/Al_2O_3 and Re/SiO_2 5 bar H_2 gas was applied and the data taken from our previous publication [19]. Data summarized in Table S1.

It should be noted that in this reaction system no H_2 gas or other additional reducing agent was added and only methanol acts as a hydrogen donor. It was also confirmed that under the applied reaction conditions H_2 is formed *in situ* by methanol decomposition [19] in the presence of Re catalyst. Moreover, methanol also serves as a protecting agent for the carboxyl groups of the reactant. Due to fast, non-catalytic esterification with the solvent, undesired side reactions such as inter- or intramolecular esterification reactions as well as hydrogenation of the carboxyl functions, which are occurring readily in non-alcoholic solvents [31], can be avoided.

Interestingly, the two Re catalysts containing acidic zeolite supports showed hardly any DODH activity (Fig. 2). While their acidity may contribute to the undesired esterification of free (mucic and muconic) acids, less than 1 % of DODH product were obtained. Thus, Re/zeolites are apparently not suitable for our reaction system, in contrast to other studies on DODH [28]. A crucial difference might either be that in that study a secondary and thus more active reducing agents was used. Moreover, the more complex nature of aldaric acids compared to the model compound allows for more undesired side reactions to occur or steric hindrances that can adversely affect the overall process. Microporous nature of zeolites also should not limit the accessibility of the reactants to the active sites, since average pore width of the most active catalyst tested (Re/C) was even smaller.

Re/ZrO_2, Re/SiO_2 and Re/Al_2O exhibited more pronounced DODH formation, with yields ranging from approximately 2–7 %. Nevertheless, activity is dramatically lower than over Re/C. Previous studies report that DODH activity of Re supported on these types of support materials often show rather comparable activity [32–34]. Re/TiO_2 was found to be the most active DODH catalyst among those with oxide support (Fig. 2), 21 % yield of dimethyl muconate were obtained as the only DODH product in this case, which is still a 2/3 lower total yield compared to Re/C, which further raises the question why this particular catalysis is so highly active. However, Tomishige [34–36] published promising results with CeO_2 support when Re was also doped with additional metal(s).

Interestingly, none of the oxide-supported Re catalysts was able to saturate double bond(s) of dimethyl muconate in significant amounts, which is in contrast to Re/C as well. The hydrogenation process is directly linked to the accessible quantity of adsorbed hydrogen, which, in turn, is correlated with the catalyst's capability to generate hydrogen from methanol. In case of the hydrogenation typically a metallic active site is required, which may be an indication that a lower amount of reduced Re species on the oxidic catalysts may play a role. It is also plausible that Rhenium undergoes rapid reoxidation in the presence of an oxidic support, whether at room temperature, after pre-reduction, or even at elevated temperatures within the reaction mixture. However, it is also conceivable that other properties such as the Re dispersion are responsible for this difference in catalytic behavior [37].

Characterization of selected catalysts was employed to understand the observed catalytic phenomena in more detail. N_2 physisorption experiments were conducted to investigate the role of textural properties and porosity. In this regard, considerable differences can be expected among the support materials included in this study.

According to IUPAC [38] Re/C, Re/H-Y zeolite and Re/H-ZSM-5 catalysts show typical IV isotherms, which are combinations of micropores with H4 hysteresis, whereas Re/SiO_2, Re/Al_2O_3, Re/ZrO_3

represent a type IV isotherm, which is a combination of micro- and mesopores with an H1 hysteresis loop type due to the presence of narrow slit mesopores (Fig. 3, Figure S2 and Table S4). While there is no indication that the textural properties of the catalysts directly affect their behavior in the catalytic DODH reaction, it is generally known that a high specific surface area can be beneficial in facilitating high metal dispersion and thus exert influence rather indirectly. To get a better insight into the size and dispersion of Re (species) in the selected catalysts, the TEM analysis of the catalysts (reduced at 400 °C with H_2 for 3 h) was conducted (Fig. 4a and b).

Re/C consists of shapeless, micron-sized C flakes decorated with ca. 50 nm-sized agglomerates of smaller nanoparticles (Fig. 4a). Closer inspection of those agglomerates revealed that they consist of small, 2 – 5 nm sized crystalline Re nanoparticles (Fig. 4b). However, EDS analysis (Figure S7) of areas on the C surface where Re nanoparticles were not visible also revealed the presence of Re and O, suggesting that additional Re or Re-oxide species are likely dispersed atomically on the carbon surface (See Fig. 8 and accompanying discussion).

All oxidic supports exhibit a notable arrangement of well-dispersed Re nanoparticles (Fig. 4c, d and ESI). In the Re/SiO_2 catalyst Re nanoparticles exist in two different size ranges. In terms of number-weighted distribution majority of Re nanoparticles are of 1.5 nm ± 0.4 nm (poorly seen in Fig. 4c) while a significant fraction of nanoparticles are uniformly distributed over the size range in between 3 nm and 12 nm (well visible in Fig. 4c) without exhibiting any maximum in number-weighted size distribution function (Figure S4). For the Re/TiO_2 sample, Re nanoparticles are of uniform size of 1.4 nm ± 0.5 nm (Figure S5) and homogeneously distributed on the surface of ca. 50 nm-sized TiO_2 nanoparticles (Fig. 4d). For the Re/Al_2O_3 sample Re nanoparticles are difficult to see because the alumina is in the form small (roughly 20 nm x 20 nm and a few nm thick) platelets that agglomerate in various orientations which results in large variation of contrast (Figure S6 a). However, induvial as well as agglomerates of Re nanoparticles are uniformly distributed over alumina. Size of Re nanoparticles is 2.0 nm ± 0.6 nm (Figure S6 a). In the sample Re/ZrO_2 Re nanoparticles are very small 0.5 nm ± 0.1 nm and uniformly distrusted over the surface of roughly 20 nm-sized ZrO_2 nanoparticles (Figure S6 b).

H_2-TPR was conducted to gain insight into the reducibility of Re on the different support materials. The obtained TPR profiles, are shown in Fig. 5. Overall, Re reduction takes place between 200 and 350 °C, which is below the temperature of the reductive pre-treatment step prior to catalytic experiments. All catalysts show a single reduction peak, indicating that probably the same reduction step is observed. However, significant differences are apparent regarding the temperature at which

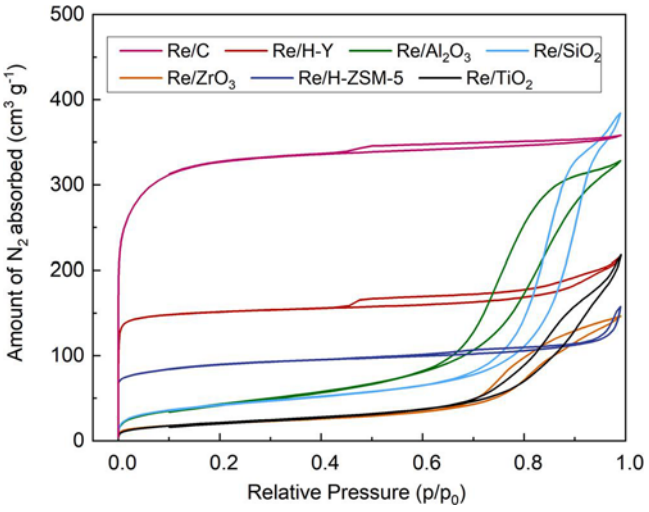

Fig. 3. Nitrogen sorption isoterms at 77 K for fresh DODH catalysts used in this study.

oxidized Re species can be reduced on the respective support material. The highest reduction temperature was observed for Re/ZrO_2 (maximum at 281 °C, entry 4 in Table 1), while the lowest found for H-ZSM-5-supported Re (230 °C, entry 2 in Table 1). The measured maximum reduction peak of Re/TiO_2 correlates very well with the values reported in the literature [39] and is comparatively low. For the most active catalyst Re/C, the maximum H_2 consumption is centered around 270 °C. Thus, there is no apparent correlation between facile Re reduction and high activity. Furthermore, the stabilization of oxidic species on Re/ZrO_2 also has no beneficial effect. Among the tested materials, Re/C and Re/ZrO_2 showed the highest hydrogen consumption, which can be seen as a measure for the amount of reducible Re species. Also this property cannot be directly correlated to the observed catalytic behaviour. However, it must be pointed out that the TPR experiments do not permit insight into the actual reduction steps and the involved Re species. Therefore, to study the oxidation state of the catalysts other methods are more suitable and allow for deeper insights into the species of Re that are present on the different catalysts.

XPS was performed for four representative catalyst samples to determine the oxidation states of Re before the catalysts were introduced into the reactor (Fig. 6). All peak positions observed agree with the standards reported in the literature [40]. A slight shift to higher binding energies (about 2 eV) was observed, probably due to the interaction of Re with the support.

Having been exposed to reductive pre-treatment under H_2 at 400 °C, all Re on the SiO_2 support was completely in metallic state (main peak at about 40.8 eV), indicating that the reductive pre-treatment was successful. In contrast, only a slight amount of partially reduced ReO_2 species (main peak at about 43.2 eV) was observed when Re was deposited on TiO_2 with most Re being present as Re^{+6} (main peak at about 45.6 eV This appears to be in contrast to the findings of the H_2-TPR experiments earlier, which indicated a facile reduction of Re on this support. However, it needs to be considered that the catalysts were exposed to air after the reductive pre-treatment during transfer to the spectrometer (similar exposure as the transfer to the reactor). Thus, TiO_2 can probably also facilitate the re-oxidation of metallic Re to Re oxide.

A very interesting observation was made when comparing Re/C before and after reduction. As expected, the unreduced catalyst (Re/C-NR) was fully oxidised, i.e., in the 6+ oxidation state (main peak at about 45.6 eV). After reduction (and subsequent exposure to air) however, both oxidized species and metallic Re were present in the sample, which indicates that both species can be stabilized by the carbon support simultaneously. It remains speculative whether there could be a correlation with the TEM findings, e.g., that both atomically dispersed Re species, which could represent Re oxide species, as well as nanoparticles (some as agglomerates), which are more likely the metallic Re species.

Previous studies, summarized e.g. by Tomishige *et al.* [24], indicate that oxidic Re species are essential for the catalytic DODH reaction. Our results show that in case of monometallic Re catalysts the presence of both oxidic and metallic Re species might be even more beneficial than primarily providing oxidic Re species. One possible explanation is that the metallic Re sites take over the role of noble metals in bimetallic DODH catalysts as described by Deng *et al.* [21] and Jang *et al.* [22,23]. The metallic sites could thus facilitate the redox cycle of the oxidic Re sites responsible for the DODH reaction by providing active hydrogen species, which likely includes facilitated dissociation of the reducing agent methanol. Based on this suggested concept of a bifunctional monometallic Re catalyst a more detailed discussion of such a reaction mechanism is provided at the end of this article.

Regarding the influence of the support material on the catalytic DODH reaction it ca be summarized that while one important function is to enable sufficient Re dispersion, the perhaps more crucial role is to stabilize Re in a suitable oxidation state or rather oxidation states. In this context, the Re/C catalyst stands out since it allows for the co-existence of bot metallic and oxidic Re species, which appears to be highly beneficial. In such a case, the balance between the two relevant species

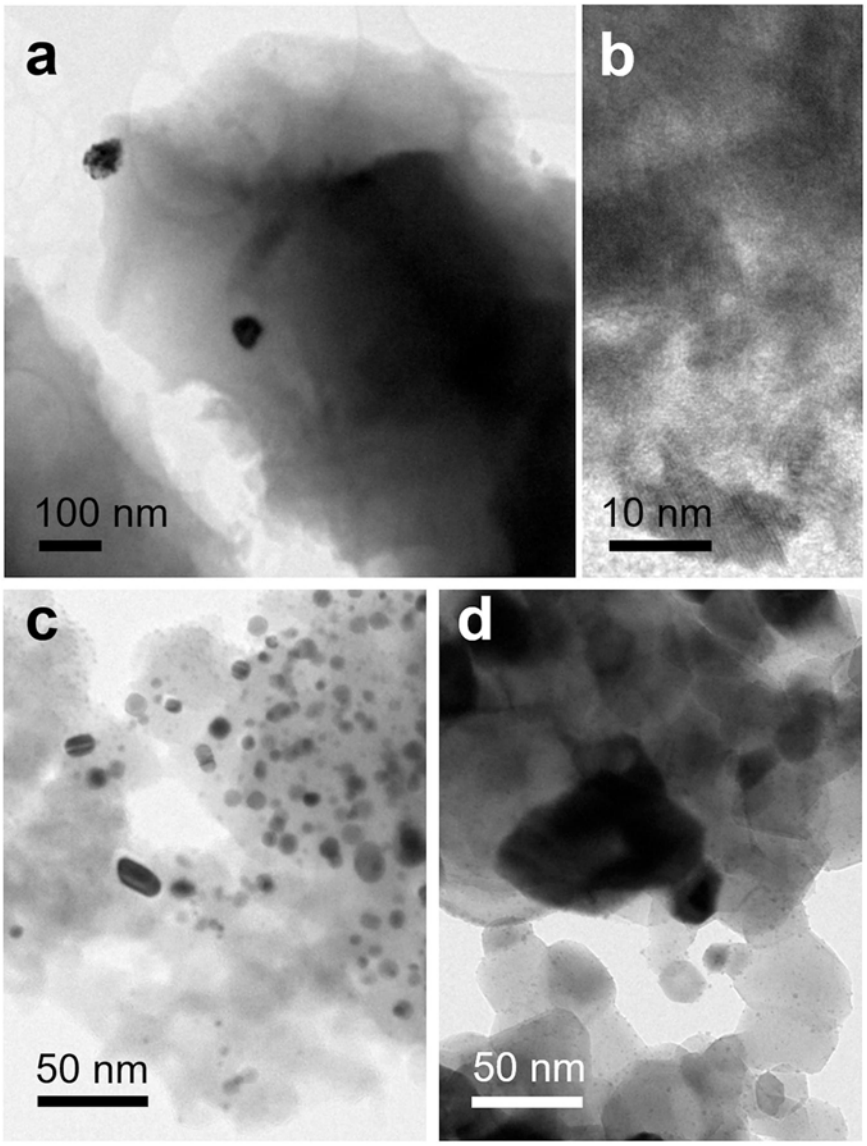

Fig. 4. TEM images of the Re/C (a), Re agglomerate in Re/C (b), Re/SiO_2 (c) and Re/TiO_2 (d) catalysts.

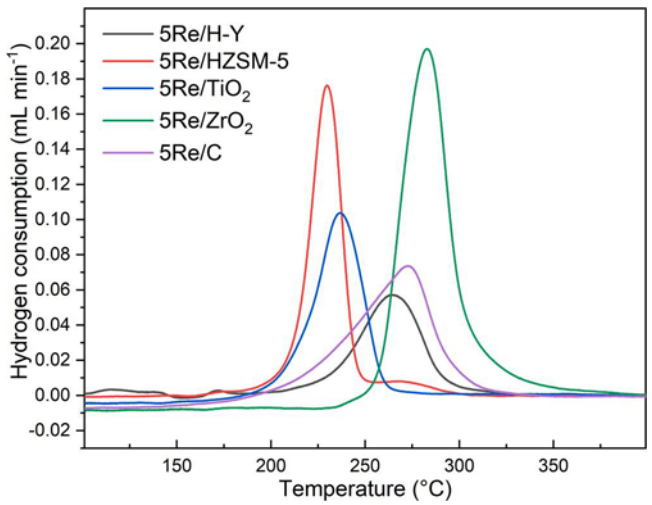

Fig. 5. H_2-TPR profiles showing temperature-dependent (5 K min^{-1}) H_2 consumption of unreduced Re-containing materials used in this work.

Table 1
Summarized H_2-TPR results of fresh (unreduced) samples.

Entry	Sample	Temperature at Maximum (°C)	H_2 uptake (cm^3/g STP)
1	Re/H-Y	265	5.4
2	Re/H-ZSM-5	230	7.6
3	Re/TiO_2	238	6.9
4	Re/ZrO_2	281	8.9
5	Re/C	270	8.4

should be among the most important factors influencing the catalytic performance of the catalyst. Therefore, by varying the reductive pre-treatment procedure it was attempted to influence this balance and learn more about the role of the different Re species. Moreover, it can help decouple the effects of changes in oxidation state and Re sintering.

3.2. *Influence of the pre-treatment conditions*

Reductive pre-treatment, employed to control the Re oxidation states and/or their distribution can potentially also influence the dispersion of Re due to sintering during the thermal treatment. Thus, it can be

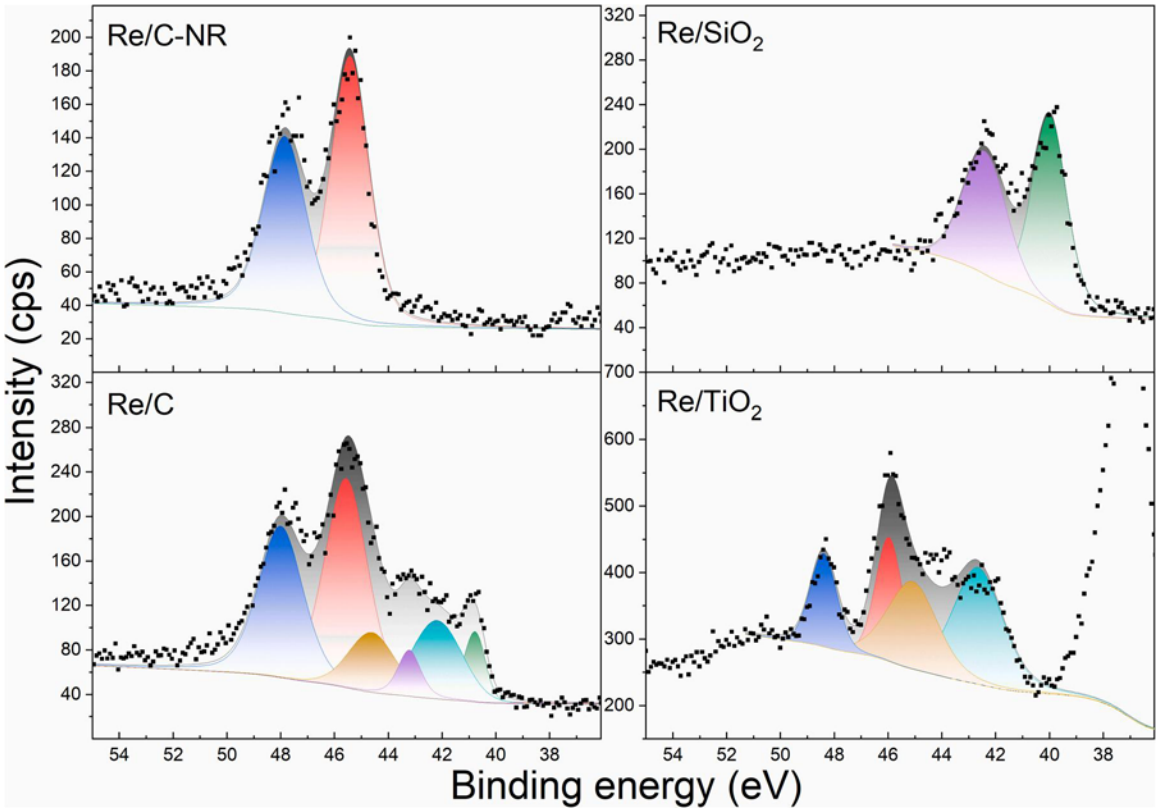

Fig. 6. XPS spectra of the Re 4 f region for the representative materials. The catalyst Re/C-NR was measured as received, while the other catalysts were reduced prior to measurement. The 4 f 7/2 peaks of ReO_3, ReO_2, and metallic Re are marked with red, cyan, and green, respectively. The 4 f 5/2 peaks of ReO_3, ReO_2, and metallic Re are marked with blue, brown, and purple, respectively.

employed to further investigate the influence of these material properties on the catalytic behavior. For Re/C, which demonstrated the highest DODH potential as indicated by the results in Fig. 2, the pre-treatment procedure was varied (Fig. 7) to decouple their respective effect on the overall catalytic activity.

The DODH of the differently treated Re/C catalyst can be best assessed from the product yields obtained after 6 h, where clear differences are apparent. At this stage of the reaction, dimethyl muconate is the predominant DODH product and hydrogenation is only observed

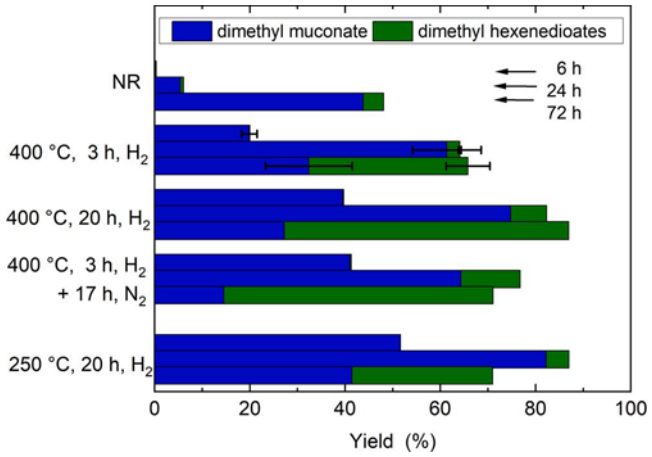

Fig. 7. Yield of dehydroxylation products after 6, 24 and 72 h obtained over Re/C exposed to different pre-treatment procedures as labelled (NR denotes non-reduced sample). Reaction conditions: 140 mg mucic acid, 45.0 mL methanol, 140 mg catalyst, 120 °C, 5 bar N_2, 72 h. Data summarized in Table S2 and reaction progress for each experiment presented in Fig. S1.

negligible amounts (<0.3 %). Over the Re/C catalyst exposed to the standard pre-treatment conditions, i.e., 3 h under H_2 at 400 °C, ca. 20 % of dimethyl muconate were formed. Prolonging the reduction time to 20 h significantly increased DODH activity and yield nearly doubled. This could be interpreted as an indication that more reduced Re is formed over the longer duration and that these reduced and perhaps metallic species contribute to the increased DODH activity. However, dimethyl muconate yield was comparable over Re/C that was pre-treated for 20 h at 400 °C first under H_2 (3 h) followed by the non-reducing gas N_2 (17 h). This rather indicates that the prolonged thermal treatment regardless the reducing gas is the more relevant factor. Sintering of Re to form more active sites could be an explanation for this behavior. Interestingly, lowering the temperature of the pre-treatment procedure to 250 °C (20 h under H_2) resulted in even higher DODH activity corresponding to >50 % dimethyl muconate yield after 6 h. This observation suggests that solely intensifying the reduction of Re during the pre-treatment procedure may not be adequate for increasing catalytic activity. According to the TPR profile of the Re/C catalyst (Fig. 5), Re reduction may not be fully reduced since the reduction maximum is at ca. 270 °C. This could have the consequence that more Re remains in high valent states compared to the samples reduced at 400 °C. Nevertheless, as reported in the literature, the Re species began displaying lower valency within the temperature range of 200–400 °C during H_2 reduction [41]. Prior to the reduction process, rhenium exists on the catalyst surface in various oxidized forms and oxidation states. According to literature findings, Re_2O_7 sublimates at a relatively low temperature of 180 °C before undergoing reduction [42]. On the other hand, it can be reduced to a more stable form, ReO_3, though this too may start decomposing at 400 °C if not further reduced to even more stable forms, such as ReO_2 or the metallic form [43]. It must be stated, however, that there is still a clear benefit of reductive pre-treatment in general, as our previous study revealed [19,43], therefore the presence

of some metallic species is beneficial.

With the further progression of the reaction, the influence of the varied pre-treatment conditions becomes less pronounced as the combined DODH yields show (Fig. 7) and the differences are barely statistically significant. However, it is apparent that the distribution of products is considerably influenced. Hydrogenation of dimethyl muconate to dimethyl hexenediolates is comparable over Re/C pre-treated under standard conditions (3 h under H_2 at 400 °C) and at lower temperature (20 h under H_2 at 250 °C). This is evident from the comparable dimethyl hexenediolate yields of approximately 30 %, underscoring the consistency in performance between the two pre-treatment approaches. Increasing the pre-treatment time to 20 h at 400 °C promotes the hydrogenation significantly and dimethyl hexenediolate yields up to ca. 60 % were obtained. For the hydrogenation reaction it appears likely that it is advantageous to promote the Re reduction to obtain more metallic Re species, which are assumed to be active in hydrogenation reactions [24].

Thus, the catalytic data suggest that during reductive pre-treatment not only the oxidation state of Re but also other properties of the catalyst must be affected, such as the Re dispersion and agglomeration. Therefore, catalyst characterization of differently pre-treated Re/C was conducted to understand the effect of the pre-treatment procedure on the material properties of the catalyst to gain insight how these affect the catalytic behavior.

STEM and TEM were employed to investigate the influence of reductive pre-treatment on the distribution of Re species on the carbon support. The unreduced Re/C catalyst shows only individual Re atoms (or clusters of Re atoms) visible only on HAADF STEM images (Fig. 8a and c) while BF images show only modest variation in contrast due to lack of crystallinity of Re species (Fig. 8b and d). No visible nanoparticles could be detected by TEM imaging as well (Fig. 8e). EDS analysis (Figure S7) performed at several locations in the sample, however, shows Re and O indicating that the C surface is covered with Re probably in the form of adsorbed Re-O_x species, as the XPS results shown above suggest as well. The reduction process at comparatively low temperature of 250 °C for 20 hours did not result in significant formation of Re nanoparticles. Most of the sample appears similar to the unreduced sample, i.e. showing no particles of Re with the exception of only a few small ca. 2 nm-sized nanoparticles (Fig. 8f). Probably the sample is rather inhomogeneous and the part that was observed with TEM shows only very low number of formed Re nanoparticles since catalytic DODH significantly increases. Considering the fact that oxidic Re species are typically considered to be the catalytically active DODH species, it seems reasonable that a high amount of these sites should be present, while the promoting effect of the reductive pretreatment could be assigned to the metallic Re sites.

In the Re/C catalyst reduced at 400 °C for 20 h a few approximately 10 nm-sized nanoparticles are formed (Fig. 8c), indicating more pronounced formation and growth of Re nanoparticles form atomically dispersed Re species. However, majority of the sample does not contain visible nanoparticles. Overall, there are agglomerates on the catalyst surface that bear a resemblance to those found on the catalyst reduced for 3 h at 400 °C in an H_2 flow, albeit smaller in size, which shows that longer reduction time leads to enhanced growth and agglomeration. Interestingly, this has a positive influence on the catalytic DODH reaction. In view of the earlier findings it appears unlikely that the formation of more metallic species at the cost of fewer oxidic Re species is causing this effect. A more likely explanation could be that the more relevant effect of the longer thermal treatment is the formation of more interfacial sites between both species. However, this is difficult to assess based on the lack of special information on the Re species in relation to the metallic nanoparticles.

Lastly, the Re/C sample pre-treated at 400 °C with H_2 for 3 h followed by N_2 appears rather homoheneously decorated with Re nanoparticles of ca. 2 nm in diameter (Fig. 8h). This catalyst had a comparable activity to the one treated for the same time under H_2, which further indicates that the potentially progressing reduction of Re is not the decisive factor. Thus, growth of Re is probably a more relevant factor, even though the underlying effects could not be fully explained.

Overall, reductive pre-treatment proves to be advantageous for the DODH reaction over Re/C as it impacts both the oxidation state of Re and induces growth. The reduction process is crucial, as metallic Re promotes DODH, likely by supplying activated hydrogen. However, DODH also depends significantly on high-valent Re. Growth, while promoting the creation of larger Re sites, also facilitates the interaction between these two types of sites. Furthermore, it is worth noting that metallic Re is crucial for the subsequent double bond hydrogenation reaction since catalysts with considerable amounts of Re nanoparticles formed during the reduction are particularly active in this regard. These finding support and enhance the model of a bifunctional Re catalyst,

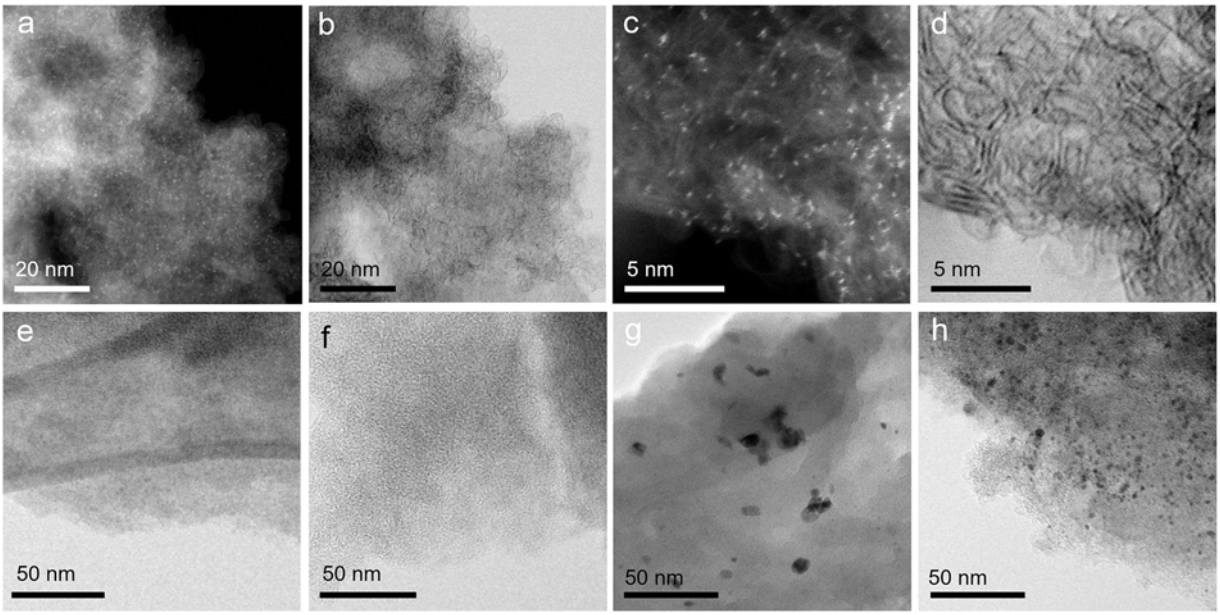

Fig. 8. STEM and TEM images of catalysts. Unreduced HAADF (a and c), BF (b and d), TEM(e), reduced at 250 °C for 20 h (f), reduced at 400 °C for 20 h (g) and reduced at 400 °C 3 h in H_2 and 17 h in N2 (h).

which is outlined next.,

3.3. Bifunctional nature of the catalyst

Based on the findings of both the support variation as well as the study of the pre-treatment effects, we propose the DODH over supported monometallic Re catalysts to critically rely on the co-existence of both metallic and high-valent Re sites. A schematic depiction is provided in Fig. 9, which relies on different Re species fulfilling different functions in the catalytic reaction.

It has been well reported that the main catalytically active species in the DODH reaction are high-valent Re sites [21,22,24], especially when combined on bimetallic catalysts with an additional noble metal providing metallic sites. However, due to the lack of an additional noble metal in the monometallic Re catalyst presented here, Re itself is suggested to also provide metallic sites at which the reducing agent (methanol) is catalytically decomposed and where activated hydrogen species are available for the DODH reaction. Especially when in the vicinity, these hydrogen species can more facilely reduce high-valent Re species than their direct reduction with methanol would allow. The low-valent Re species, which are more readily formed in this process, play a crucial role as intermediates in the catalytic DODH cycle [16,24]. These species have the ability to interact with vicinal diols, making selective dehydroxylation feasible. Consequently, the catalytic reaction exhibits a bifunctional nature, relying on both metallic and high-valent oxidic Re sites, as illustrated in Fig. 9a.

As the experimental results indicate, two aspects are essential in governing catalytic DODH activity over these bifunctional Re catalysts: Firstly, both types of active Re sites must be present and their balance is crucial. Therefore, the role of the support material is to enable this balance by stabilizing the co-existence of both species, also under reaction conditions. Reductive pre-treatment is important to generate metallic species in the first place, however over-reduction and thus imbalance must be avoided. Secondly, both metallic and high-valent Re sites must be able to interact. The effect of thermal treatment that leads to the formation of Re agglomerates can likely increase the probability of forming bifunctional sites. However, it is also possible that a redox-active support material can play a mediating role and bridge the gap between the two sites. Overall, the observed experimental data regarding the DODH activity align well with the bifunctional mechanism proposed.

An additional aspect in the overall reaction of mucic acid towards adipates is the occurrence of consecutive hydrogenation reactions. fi Thus, pre-treatment conditions that favor the formation of metallic Re species lead to catalysts that are able to catalyze also the hydrogenation of dimethyl muconate to dimethyl hexenedioates. Nevertheless, it appears that Re alone may not catalyze the complete hydrogenation to adipates unless more rigorous reaction conditions are employed [19], or an external source of hydrogen is introduced. For faster hydrogenation, the use of an additional hydrogenation catalyst materials, such as Pd or Pt, proves to be clearly advantageous [44].

4. Conclusions

In this study, the selective DODH followed by the hydrogenation of biobased aldaric acid to adipic acid esters was effectively conducted, yielding upto 88 % DODH products through the use of a Re catalyst on a carbon support under mild conditions (120 °C in methanol). Notably, alternative supports such as oxides like TiO_2 and SiO_2, as well as zeolites, demonstrated considerably lower activity. Characterization showed that while the oxidic supports primarily contained either primarily metallic (SiO_2) or high-valent Re species (TiO_2), different Re species co-exist on the carbon support. Thus, the stabilization of different Re species, as well as providing high Re dispersion, are probably what makes carbon an ideal support for the DODH reaction. The reasons for superior suitability of C as a support can be found in specific electronic effects that keep Re in several oxidation states combined with hydrophobic nature of the support repelling H_2O products and attraction of a non-polar H_2 molecules or eventual gaseous phase formed.

Moreover, adjusting the properties of Re/C prior to the catalytic reaction can be achieved by reductive pre-treatment, which significantly influences also the catalytic performance. While reduction in general is necessary to generate metallic Re sites, particulate growth of Re probably also contributes to enhanced catalytic activity by promoting the formation of bifunctional sites. The highest DODH activity was obtained by long pre-treatment at 250 °C, indicating that higher temperatures may lead to over-reduction of the catalyst by reducing the number of high-valent Re sites.

The findings were combined to propose a bifunctional catalytic DODH mechanism of the monometallic Re/C catalyst, which has both metallic and higher-valent Re sites. Metallic Re sites are suggested to promote the decomposition of methanol and provide activated hydrogen species, which facilitate the reduction of high-valent Re species during the catalytic DODH cycle. The thus formed low-valent Re species can reductively dehydroxylate the reactant mucic acid (methyl ester) via double bond formation, which is the essential step of the DODH reaction. Thus, the reaction depends on the vicinity of both reduced and high-valent Re species forming a bifunctional active site. Overall, the balance of both Re sites is crucial and sintering due to thermal pre-treatment may enhance the formation of bifunctional sites. In addition, metallic Re sites also catalyze the hydrogenation of the double bonds to form partially saturated products. Full hydrogenation to

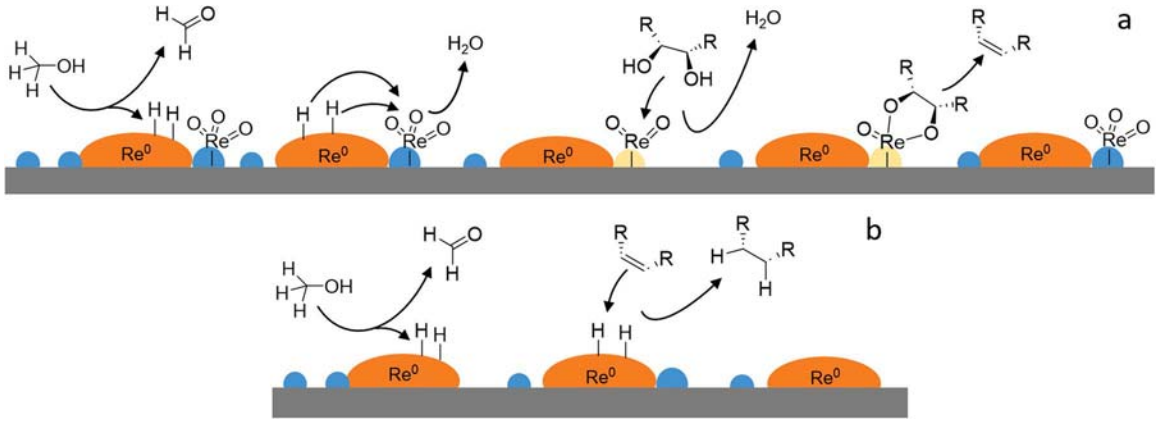

Fig. 9. a) Possible interplay of metallic (orange) and high-valent (blue) Re sites on the Re/C catalyst enabling the concerted formation of activated hydrogen species and deoxydehydration reaction on the respective sites. During the deoxydehydration cycle the Re site must be first reduced (to a low-valent Re site, yellow) and later re-oxidized, as suggested in [16,24]. b) The subsequent hydrogenation reaction requires metallic Re sites.

adipates, however, was not observed under the mild reaction conditions.

CRediT authorship contribution statement

Janvit Teržan: Writing – original draft, Visualization, Methodology, Investigation, Conceptualization. **Maja Gabrič:** Writing – review & editing, Writing – original draft, Methodology, Investigation, Data curation. **Brigita Hočevar:** Writing – review & editing, Supervision, Methodology, Funding acquisition. **Miha Grilc:** Writing – review & editing, Supervision, Project administration, Methodology, Funding acquisition, Conceptualization. **Blaž Likozar:** Supervision, Project administration, Funding acquisition, Formal analysis, Conceptualization. **Sašo Gyergyek:** Writing – original draft, Visualization, Investigation, Data curation. **Florian M. Harth:** Writing – review & editing, Writing – original draft, Methodology, Investigation, Conceptualization.

Declaration of Competing Interest

The authors declare that they have no known competing financial interests or personal relationships that could have appeared to influence the work reported in this paper.

Data availability

Data will be made available on request.

Acknowledgement

This research was funded by the Slovenian Research and Innovation Agency (research projects N2–0242 and J1–3020 and research core funding P2–0152). Nives Kokol, Anej Blažič, Urška Kavčič and Vili Resnik are acknowledged for their excellent experimental and moral support.

Appendix A. Supporting information

Supplementary data associated with this article can be found in the online version at doi:10.1016/j.cattod.2024.114879.

References

[1] N. Dahmen, I. Lewandowski, S. Zibek, A. Weidtmann, Integrated lignocellulosic value chains in a growing bioeconomy: Status quo and perspectives, GCB Bioenergy 11 (2019) 107–117, https://doi.org/10.1111/gcbb.12586.
[2] J.A. Okolie, A. Mukherjee, S. Nanda, A.K. Dalai, J.A. Kozinski, Next-generation biofuels and platform biochemicals from lignocellulosic biomass, Int. J. Energy Res. 45 (2021) 14145–14169, https://doi.org/10.1002/er.6697.
[3] J.-P. Lange, Lignocellulose conversion: an introduction to chemistry, process and economics, Biofuels, Bioprod. Bioref. 1 (2007) 39–48, https://doi.org/10.1002/bbb.7.
[4] H. Kobayashi, H. Ohta, A. Fukuoka, Conversion of lignocellulose into renewable chemicals by heterogeneous catalysis, Catal. Sci. Technol. 2 (2012) 869–883, https://doi.org/10.1039/c2cy00500j.
[5] D. Haldar, M.K. Purkait, Lignocellulosic conversion into value-added products: A review, Process Biochem. 89 (2020) 110–133, https://doi.org/10.1016/j.procbio.2019.10.001.
[6] P. Gallezot, Conversion of biomass to selected chemical products, Chem. Soc. Rev. 41 (2012) 1538–1558, https://doi.org/10.1039/c1cs15147a.
[7] I. Delidovich, P.J.C. Hausoul, L. Deng, R. Pfützenreuter, M. Rose, R. Palkovits, Alternative Monomers Based on Lignocellulose and Their Use for Polymer Production, Chem. Rev. 116 (2016) 1540–1599, https://doi.org/10.1021/acs.chemrev.5b00354.
[8] F.H. Isikgor, C.R. Becer, Lignocellulosic biomass: a sustainable platform for the production of bio-based chemicals and polymers, Polym. Chem. 6 (2015) 4497–4559, https://doi.org/10.1039/C5PY00263J.
[9] J.-G. Rosenboom, R. Langer, G. Traverso, Bioplastics for a circular economy, Nat. Rev. Mater. 7 (2022) 117–137, https://doi.org/10.1038/s41578-021-00407-8.
[10] J.C.J. Bart, S. Cavallaro, Transiting from adipic acid to bioadipic acid. Part II. Biosynthetic pathways, Ind. Eng. Chem. Res. 54 (2015) 567–576, https://doi.org/10.1021/ie502074d.
[11] Y. Deng, L. Ma, Y. Mao, Biological production of adipic acid from renewable substrates: Current and future methods, Biochem. Eng. J. 105 (2016) 16–26, https://doi.org/10.1016/j.bej.2015.08.015.
[12] J. Rios, J. Lebeau, T. Yang, S. Li, M.D. Lynch, A critical review on the progress and challenges to a more sustainable, cost competitive synthesis of adipic acid, Green. Chem. 23 (2021) 3172–3190, https://doi.org/10.1039/d1gc00638j.
[13] M. Lang, H. Li, Sustainable routes for the synthesis of renewable adipic acid from biomass derivatives, ChemSusChem 15 (2022) e202101531, https://doi.org/10.1002/cssc.202101531.
[14] F.C. Jentoft, Transition metal-catalyzed deoxydehydration: missing pieces of the puzzle, Catal. Sci. Technol. (2022), https://doi.org/10.1039/D1CY02083H.
[15] J.R. Dethlefsen, P. Fristrup, Rhenium-catalyzed deoxydehydration of diols and polyols, ChemSusChem 8 (2015) 767–775, https://doi.org/10.1002/cssc.201402987.
[16] M. Shiramizu, F.D. Toste, Deoxygenation of biomass-derived feedstocks: Oxorhenium-catalyzed deoxydehydration of sugars and sugar alcohols, Angew. Chem. - Int. Ed. 51 (2012) 8082–8086, https://doi.org/10.1002/anie.201203877.
[17] M. Shiramizu, F.D. Toste, Expanding the scope of biomass-derived chemicals through tandem reactions based on oxorhenium-catalyzed deoxydehydration, Angew. Chem. - Int. Ed. 52 (2013) 12905–12909, https://doi.org/10.1002/anie.201307564.
[18] B. Hočevar, B. Likozar, M. Grilc, 2021, B. Hočevar, B. Likozar, M. Grilc, Sustainable process for producing muconic, hexenedioic and adipic acid (and their esters) from aldaric acids by heterogeneous catalysis, EP3782976A1, 2021..
[19] B. Hočevar, A. Prašnikar, M. Huš, M. Grilc, B. Likozar, H 2-Free Re-Based catalytic dehydroxylation of aldaric acid to muconic and adipic acid esters, Angew. Chem. Int. Ed. 60 (2021) 1244–1253, https://doi.org/10.1002/anie.202010035.
[20] J. Lin, H. Song, X. Shen, B. Wang, S. Xie, W. Deng, D. Wu, Q. Zhang, Y. Wang, Zirconia-supported rhenium oxide as an efficient catalyst for the synthesis of biomass-based adipic acid ester, Chem. Commun. 55 (2019) 11017–11020, https://doi.org/10.1039/c9cc05413h.
[21] W. Deng, L. Yan, B. Wang, Q. Zhang, H. Song, S. Wang, Q. Zhang, Y. Wang, Efficient catalysts for the green synthesis of adipic acid from biomass, Angew. Chem. Int. Ed. 60 (2021) 4712–4719, https://doi.org/10.1002/anie.202013843.
[22] J.H. Jang, I. Ro, P. Christopher, M.M. Abu-Omar, A Heterogeneous Pt-ReOx/C catalyst for making renewable adipates in one step from sugar acids, ACS Catal. 11 (2021) 95–109, https://doi.org/10.1021/acscatal.0c04158.
[23] J.H. Jang, J.T. Hopper, I. Ro, P. Christopher, M.M. Abu-Omar, One-step production of renewable adipic acid esters from mucic acid over an Ir–ReOx/C catalyst with low Ir loading, Catal. Sci. Technol. 13 (2023) 714–725, https://doi.org/10.1039/D2CY01144A.
[24] K. Tomishige, Y. Nakagawa, M. Tamura, Taming heterogeneous rhenium catalysis for the production of biomass-derived chemicals, Chin. Chem. Lett. 31 (2020) 1071–1077, https://doi.org/10.1016/j.cclet.2019.07.014.
[25] L. Sandbrink, E. Klindtworth, H.U. Islam, A.M. Beale, R. Palkovits, ReOx/TiO2: A Recyclable Solid Catalyst for Deoxydehydration, ACS Catal. 6 (2016) 677–680, https://doi.org/10.1021/acscatal.5b01936.
[26] T. Wang, Y. Nakagawa, M. Tamura, K. Okumura, K. Tomishige, Tungsten–zirconia-supported rhenium catalyst combined with a deoxydehydration catalyst for the one-pot synthesis of 1,4-butanediol from 1,4-anhydroerythritol, React. Chem. Eng. 5 (2020) 1237–1250, https://doi.org/10.1039/D0RE00085J.
[27] T. Wang, M. Tamura, Y. Nakagawa, K. Tomishige, Preparation of Highly Active Monometallic Rhenium Catalysts for Selective Synthesis of 1,4-Butanediol from 1,4-Anhydroerythritol, ChemSusChem 12 (2019) 3615–3626, https://doi.org/10.1002/cssc.201900900.
[28] I. Meiners, Y. Louven, R. Palkovits, Zeolite-supported rhenium catalysts for the deoxydehydration of 1,2-Hexanediol to 1-Hexene, ChemCatChem 13 (2021) 2393–2397, https://doi.org/10.1002/cctc.202100277.
[29] B.E. Sharkey, A.L. Denning, F.C. Jentoft, R. Gangadhara, T.V. Gopaladasu, K. M. Nicholas, New solid oxo-rhenium and oxo-molybdenum catalysts for the deoxydehydration of glycols to olefins, Catal. Today 310 (2018) 86–93, https://doi.org/10.1016/j.cattod.2017.05.090.
[30] Y. Jeong, C.W. Park, Y.-K. Park, J.-M. Ha, Y. Jeong, K.-Y. Lee, J. Jae, Investigation of the activity and selectivity of supported rhenium catalysts for the hydrodeoxygenation of 2-methoxyphenol, Catal. Today 375 (2021) 164–173, https://doi.org/10.1016/j.cattod.2020.05.004.
[31] B. Hočevar, M. Grilc, B. Likozar, Aqueous dehydration, hydrogenation and hydrodeoxygenation reactions of bio-based mucic acid over Ni, NiMo, Pt, Rh, and Ru on neutral or acidic catalyst supports, Catalysts 9 (2019) 286, https://doi.org/10.3390/catal9030286.
[32] J. Lin, H. Song, X. Shen, B. Wang, S. Xie, W. Deng, D. Wu, Q. Zhang, Y. Wang, Zirconia-supported rhenium oxide as an efficient catalyst for the synthesis of biomass-based adipic acid ester, Chem. Commun. 55 (2019) 11017–11020, https://doi.org/10.1039/c9cc05413h.
[33] B.E. Sharkey, A.L. Denning, F.C. Jentoft, R. Gangadhara, T.V. Gopaladasu, K. M. Nicholas, New solid oxo-rhenium and oxo-molybdenum catalysts for the deoxydehydration of glycols to olefins, Catal. Today 310 (2018) 86–93, https://doi.org/10.1016/j.cattod.2017.05.090.
[34] N. Ota, M. Tamura, Y. Nakagawa, K. Okumura, K. Tomishige, Hydrodeoxygenation of Vicinal OH Groups over Heterogeneous Rhenium Catalyst Promoted by Palladium and Ceria Support, Angew. Chem. Int. Ed. 54 (2015) 1897–1900, https://doi.org/10.1002/anie.201410352.
[35] S. Tazawa, N. Ota, M. Tamura, Y. Nakagawa, K. Okumura, K. Tomishige, Deoxydehydration with Molecular Hydrogen over Ceria-Supported Rhenium Catalyst with Gold Promoter, ACS Catal. 6 (2016) 6393–6397, https://doi.org/10.1021/acscatal.6b01864.
[36] K. Yamaguchi, J. Cao, M. Betchaku, Y. Nakagawa, M. Tamura, A. Nakayama, M. Yabushita, K. Tomishige, Deoxydehydration of biomass-derived polyols over

silver-modified ceria-supported rhenium catalyst with molecular hydrogen, ChemSusChem 15 (2022) e202102663, https://doi.org/10.1002/cssc.202102663.
[37] J. Okal, L. Kępiński, L. Krajczyk, W. Tylus, Oxidation and redispersion of a low-loaded Re/γ-Al2O3 catalyst, J. Catal. 219 (2003) 362–371, https://doi.org/10.1016/S0021-9517(03)00165-9.
[38] F. Ambroz, T.J. Macdonald, V. Martis, I.P. Parkin, Evaluation of the BET Theory for the Characterization of Meso and Microporous MOFs, Small Methods 2 (2018) 1800173, https://doi.org/10.1002/smtd.201800173.
[39] B. Mitra, X. Gao, I.E. Wachs, A.M. Hirt, G. Deo, Characterization of supported rhenium oxide catalysts: effect of loading, support and additives, Phys. Chem. Chem. Phys. 3 (2001) 1144–1152, https://doi.org/10.1039/B007381O.
[40] A.K.-V. Alexander, V. Naumkin Stephen, W. Gaarenstroom, and Cedric J. Powell, X-ray Photoelectron Spectroscopy Database XPS,Version 4.1, NIST Standard Reference, Database 20 (1989), https://doi.org/10.18434/T4T88K.
[41] K.W. Ting, S. Mine, A. Ait El Fakir, P. Du, L. Li, S.M.A.H. Siddiki, T. Toyao, K. Shimizu, The reducibility and oxidation states of oxide-supported rhenium: experimental and theoretical investigations, Phys. Chem. Chem. Phys. 24 (2022) 28621–28631, https://doi.org/10.1039/D2CP04784E.
[42] C. Bolivar, H. Charcosset, R. Frety, M. Primet, L. Tournayan, C. Betizeau, G. Leclercq, R. Maurel, Platinum-rhenium/alumina catalysts: I. Investigation of reduction by hydrogen, J. Catal. 39 (1975) 249–259, https://doi.org/10.1016/0021-9517(75)90329-2.
[43] R. Bacchiocchi, J. De Maron, T. Tabanelli, D. Bianchi, F. Cavani, Supported rhenium catalysts for the hydrogenation of levulinic acid derivatives: limits and potential, Sustain. Energy Fuels 7 (2023) 671–681, https://doi.org/10.1039/D2SE01583H.
[44] K. Liu, R. Qin, N. Zheng, Insights into the interfacial effects in heterogeneous metal nanocatalysts toward selective hydrogenation, J. Am. Chem. Soc. 143 (2021) 4483–4499, https://doi.org/10.1021/jacs.0c13185.